AFCRL-63-798

SEL-63-123

On the Determination of Temperature and Ionic Composition by Electron Backscattering from the Ionosphere and Magnetosphere

by

D. R. Moorcroft

October 1963

Scientific Report No. 1

Prepared under
National Aeronautics and Space Administration
Grant NsG-377, and

Scientific Report No. 7

Prepared under
U.S. Air Force Contract AF19(604)-7436
Project 5629, Task 562901
for Air Force Cambridge Research Laboratories
Office of Aerospace Research
United States Air Force
Bedford, Massachusetts

RADIOSCIENCE LABORATORY

STANFORD ELECTRONICS LABORATORIES

STANFORD UNIVERSITY · STANFORD, CALIFORNIA

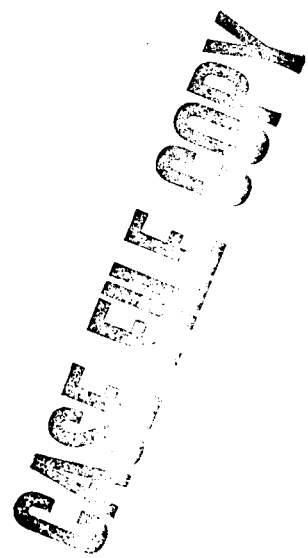

DDC AVAILABILITY NOTICES

Requests for additional copies by Agencies of the Department of Defense, their contractors, and other Government Agencies should be directed to

Defense Documentation Center (DDC)
Cameron Station
Alexandria, Virginia

Department of Defense contractors must be established for DDC services or have their "need-to-know" certified by the cognizant military agency of their project or contract.

All other persons and organizations should apply to the

U.S. Department of Commerce
Office of Technical Services
Washington 25, D.C.

(NASA CR - - -)

AFCRL-63-798)

SEL-63-125)

ON THE DETERMINATION OF TEMPERATURE AND IONIC COMPOSITION BY ELECTRON BACKSCATTERING FROM THE IONOSPHERE AND MAGNETOSPHERE

Scientific Reports Nos. 1 and 7

by

D. R. Moorcroft

October 1963

Scientific Report No. 1
Prepared under
National Aeronautics and Space Administration (NASA) Grant NsG-377)
and
Scientific Report No. 7
Prepared under
U. S. Air Force Contract AF19(604)-7436)
for
Air Force Cambridge Research Laboratories
Office of Aerospace Research
United States Air Force
Bedford, Massachusetts

3 Radioscience Laboratory
Stanford Electronics Laboratories
1 Stanford University Stanford, California 2

8249000

ABSTRACT

14842

Observations of the scattering of electromagnetic waves from thermal fluctuations in the electron density of the ionosphere and magnetosphere have previously been used to investigate ion and electron temperatures and the electron density. This work was based on the assumptions that the only ions present were O^+, and that $kD = 4\pi D/\lambda_T \ll 1$ (λ_T is the transmitted wavelength and D is the Debye length). These conditions usually apply at F-region heights.

In this paper the interpretation of such scattering is extended to conditions likely to apply above the F region, where increasing percentages of He^+ and H^+ are expected to occur, and where kD may not be very small. Detailed curves are presented for mixtures of O^+ and He^+. It appears that, with a sufficiently powerful radar operating at a sufficiently low frequency, scatter observations alone can usually be used to determine the relative concentrations of O^+ and He^+ (and/or H^+), as well as the electron and ion temperatures and the electron density. When information on one or more of these ionospheric properties is available from another source, simpler scatter observations can be used to complete the set. A simple transformation is given which accurately corrects the interpretation for values of kD up to unity.

AUTHOR

CONTENTS

ILLUSTRATIONS

ACKNOWLEDGMENTS

The author would like to acknowledge the benefit of many discussions with Prof. Von R. Eshleman during the course of this work. This work was sponsored by the National Aeronautics and Space Administration under Research Grant No. NsG-377, and by the Air Force Cambridge Research Laboratories under contract AF19(604)-7436. The use of the facilities of the Computation Center of Stanford University was supported in part by the National Science Foundation under Grant No. NSF-GP948.

I. INTRODUCTION

Observations of the scattering of electromagnetic waves from thermal fluctuations in the electron density of an ionized gas give information about the temperatures of the ions and electrons, and about the electron density. Several workers have already used this technique in the study of the upper atmosphere to determine temperatures [for example, Refs. 1, 2] and electron densities [for example, Refs. 3, 4]. The observations have been interpreted on the assumption that only one type of ion was present and the Debye length was much less than the transmitted wavelength. As ionospheric measurements are extended to greater and greater heights, the Debye length may no longer be negligible in comparison with vhf and uhf wavelengths, and there is reason to expect the ionic composition to change from O^+ at F-region heights to mixtures containing increasing amounts of He^+ and H^+. There is, therefore, a practical need to examine the spectra that arise when more than one type of ion is present, and when the Debye length is not necessarily small compared to the wavelength. In the past some attention has been paid to the possibility of using the ion gyro peaks that were predicted in the spectra for propagation nearly perpendicular to the earth's magnetic field, to identify the types and abundances of the ions present [Refs. 5-7]. So far, observations of this type have failed to reveal these ion gyro peaks [Ref. 8].

Little attention has been paid to the effects of ionic composition on the non-magnetic spectrum, which is relevant for all directions of propagation except those nearly perpendicular to the magnetic field lines. Fejer [Ref. 6] has given examples of spectra for a mixture of H^+ and O^+ when the ions and electrons have the same temperature, and Carru et al [Ref. 9] have also considered some of the effects of ionic mixtures for equilibrium conditions. In this paper the effects of ionic composition and temperature non-equilibrium on the non-magnetic spectrum will be considered in some detail. It appears that observations of this type of scattering, either alone or combined with other measurements, will provide a useful technique for the determination of the ionic composition and temperature of the upper atmosphere.

In the first part of this paper it is assumed that the Debye length is very small compared with the wavelength; precisely, it is assumed that $kD = (4\pi/\lambda_T)D \ll 1$, where λ_T is the transmitted wavelength and D is the Debye length in the scattering region. On the basis of this assumption, the interpretation when one, two, and three kinds of ions are present are examined in turn, with emphasis on mixtures of O^+, He^+, and H^+. Because of the increased complexity of the problem, only a brief discussion is given of gases containing three kinds of ions. Finally, we consider the modifications introduced when kD is not very small.

Because the treatment of a ternary mixture is so difficult, it is important to estimate over how much of the upper atmosphere such a mixture could be approximated by a binary mixture. For this purpose we have some isothermal, diffusive-equilibrium models suggested by Bauer [Ref. 10]. The distributions for temperatures of 800 ^{o}K and 1600 ^{o}K are shown in Fig. 1. As indicated at the right of each diagram, the three ions O^+, He^+, and H^+ are simultaneously present in appreciable quantities over only a relatively small range of height. At lower heights it is sufficient to consider only O^+ and He^+; at greater heights it is sufficient to consider only He^+ and H^+. Below 400 or 500 km the ions are almost exclusively O^+. It therefore appears that binary mixtures may adequately describe the ionic composition of a large part of the upper atmosphere. Accordingly, most of the emphasis in this paper is on binary mixtures of O^+ and He^+. Throughout we make the reasonable assumption that the different types of ions have the same temperature, which may, however, be different from the electron temperature.

It should be kept in mind throughout this paper that the analysis assumes that the constituent ions are known, but their relative concentrations are not. With appropriate measurements it is also possible to identify unknown ions, but such types of analysis are not considered in this paper.

The theoretical expressions for scattering from the thermal fluctuations in an ionized gas are available in various forms in several places in the literature [see, for example, Ref. 6]. For the computations in

this paper, modified forms of Fejer's expressions have been used. Many of the calculations are programmed and run on the IBM 7090 computer at Stanford University.

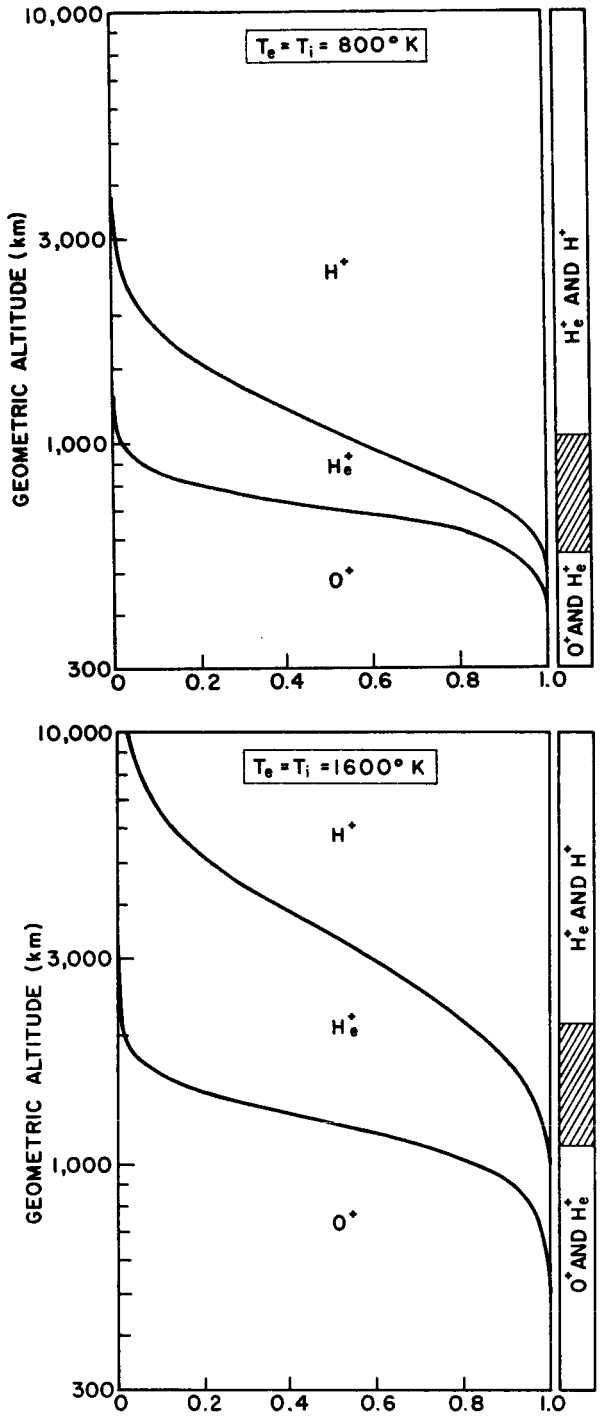

FIG. 1. RELATIVE IONIC COMPOSITION OF UPPER ATMOSPHERE FOR TEMPERATURES OF 800 AND 1600 °K. Based on isothermal, diffusive-equilibrium models of Bauer [Ref. 10].

II. AN IONIZED GAS CONTAINING ONE TYPE OF ION

The interpretation of the scattering from an ionized gas containing only one type of ion is reviewed first, since it provides a useful background against which to consider the more complicated situations. The salient features of the scattered spectrum can be seen in Fig. 2, which shows spectra for scatter from ionized gases where the ion present is oxygen, helium, or hydrogen, for electron-ion temperature ratios T_e/T_i, of 1.0, 2.0, and 3.0. Since the spectrum is symmetric about the transmitted frequency, only the half above the central (transmitted) frequency is shown. The scales for power spectral density and doppler shift f could be chosen from a large number of possibilities, depending on which quantities one wishes to incorporate into the coordinates. With the choice used here, the areas under the different curves are proportional to the scattered power. Also, the position of the peak in the spectrum for any particular ion remains in almost the same position for different electron-ion temperature ratios. (Compare this with Fejer [Ref. 6] or Evans [Ref. 1] where the position of the peak moves with a change in T_e/T_i, because of a different choice of abscissa.) The width of the spectrum is nearly proportional to the square root of the ion mass, being twice as wide for He^+ as for O^+, and twice as wide for H^+ as for He^+. Since the shape of the spectrum is of particular interest, we multiply the abscissa by the square root of the ion-electron mass ratio m_i/m_e, normalize each curve to unity at zero doppler shift, and obtain Fig. 3, which shows the spectra of Fig. 2 on these new scales. It is clear from this figure that the shape of the spectrum is only slightly dependent on the mass of the ion present in the gas.

When only one type of ion is present, and it is known, the basic approach is straightforward. The width of the spectrum Δf is proportional to the square root of the temperature, and the power scattered per unit volume σ is proportional to the electron density N. The approach is slightly complicated by the fact that in the ionosphere the electrons are often hotter than the ions. The constants of proportionality $\Delta f/\sqrt{T}$ and σ/N, then depend on the temperature ratio T_e/T_i. However, the height of the peak in the spectrum, relative to the central

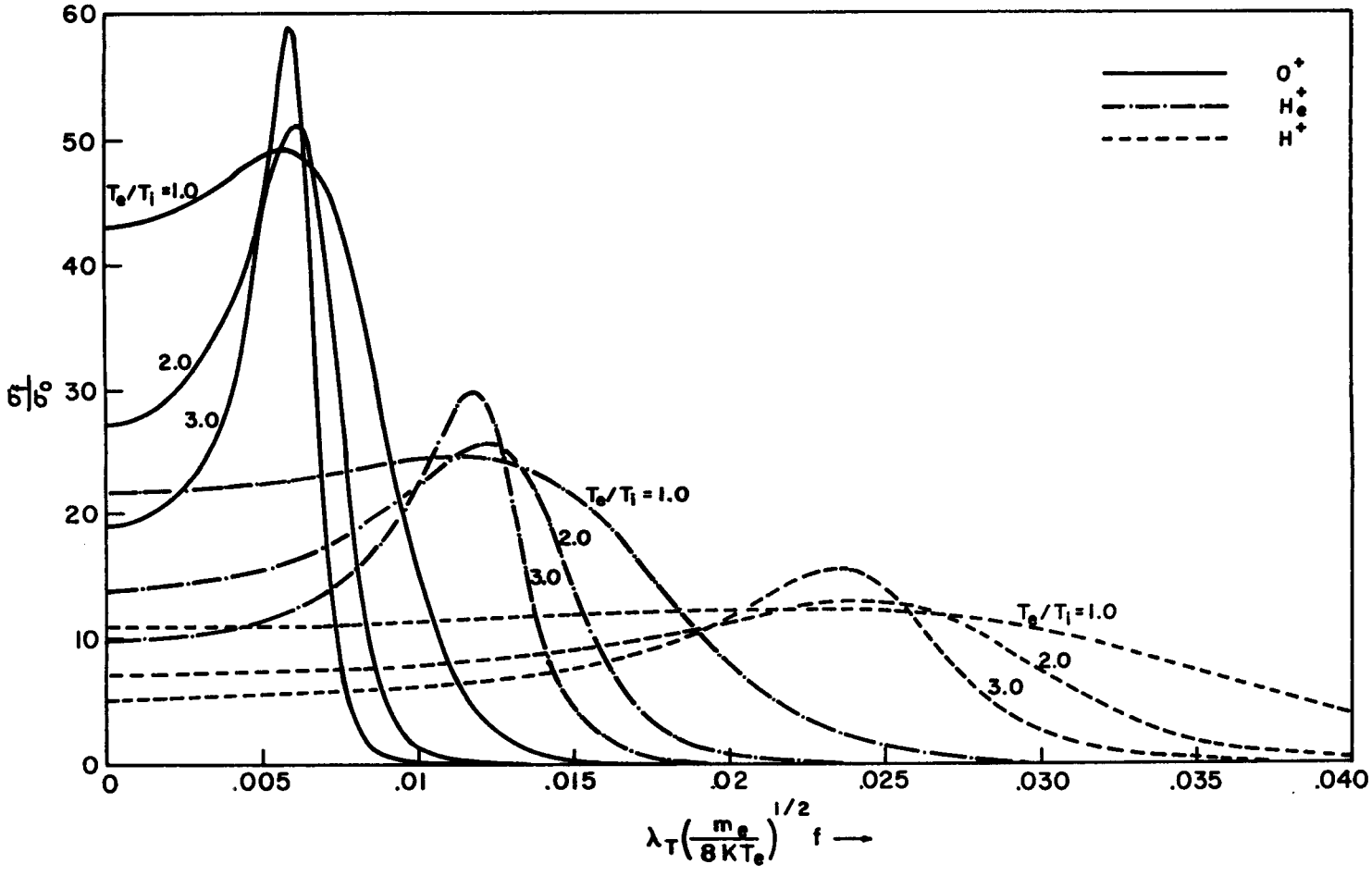

FIG. 2. SCATTER SPECTRA FOR ELECTRON-ION TEMPERATURE RATIOS OF 1.0, 2.0, AND 3.0 FOR 0^+, He^+, AND H^+. The ordinate is power spectral density, normalized by

$$\sigma_o = \lambda_T\left(\frac{m_e}{8\pi KT_e}\right)^{1/2},$$

the power spectral density at zero doppler shift in the absence of electron-ion interactions (free electron scatter). Here, λ_T is the transmitted wavelength, m_e is the mass of an electron, K is Boltzmann's constant, T_e is the electron temperature, and f is the doppler shift.

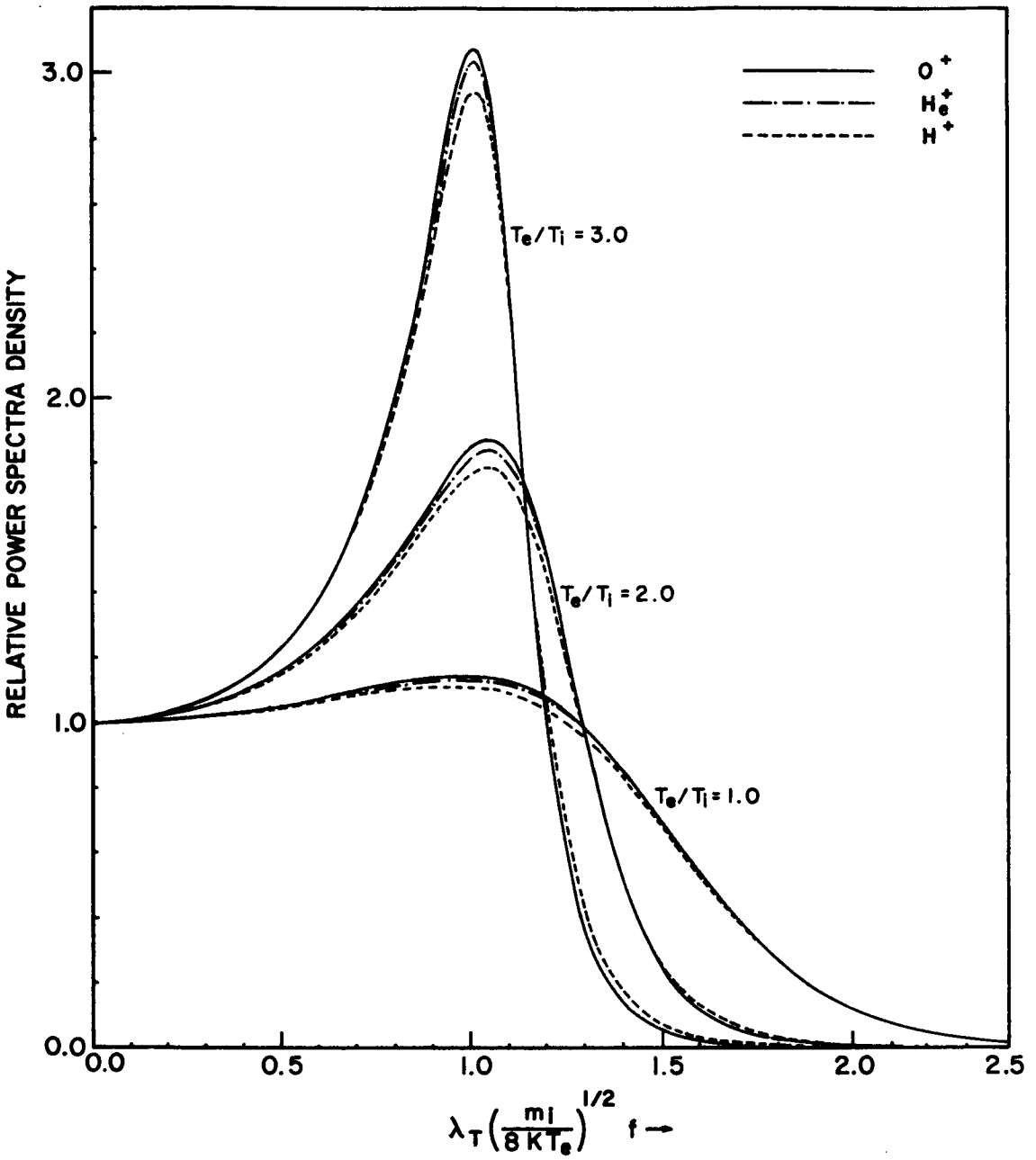

FIG. 3. SAME SPECTRA AS IN FIG. 2, BUT WITH DIFFERENT SCALES FOR ORDINATE AND ABSCISSA. Power spectral density is normalized to unity at zero doppler shift for each curve.

value R is a function only of the temperature ratio; therefore, a measurement of this ratio determines the temperature ratio, and thus the values of $\Delta f/\sqrt{T}$ and σ/N.

These various dependencies are illustrated quantitatively for the three ions O^+, He^+, and H^+ in Figs. 4, 5, and 6. In Fig. 4 the peak-to-center ratio R is shown as a function of T_e/T_i for temperature ratios from 1.0 to 3.0. (This appears to be the range of T_e/T_i appropriate for the upper atmosphere.) As might be expected from the spectra of Fig. 3, a change in the ion mass changes the value of R only slightly. In interpreting his spectral observations of scattering from F-region heights, Evans [Ref. 1] used this ratio R to deduce temperature ratios.

From many possible definitions of Δf we have selected the one used by Evans: Δf is the doppler shift at which the power spectral density falls to half of its value at the peak. Figure 5 shows the ratios $\Delta f/\sqrt{T_i}$ and $\Delta f/\sqrt{T_e}$ as functions of T_e/T_i. The figure indicates that $\sqrt{m_i}\,\Delta f$ is nearly independent of the ion mass.

It can be seen from Fig. 1 that the ratio σ/N is a function of T_e/T_i, since the areas under the spectra are proportional to σ. It is also slightly dependent on the ion mass [Ref. 11]. These dependencies are shown in Fig. 6 for O^+, He^+, and H^+.

If all three of the quantities R, Δf, and σ can be measured, it is possible to determine T_e, T_i, and N, using the curves of Figs. 4, 5, and 6. If not all of these scattering quantities can be measured, it may be necessary to make some assumptions about the temperatures, or perhaps make a measurement of N in another way. The various combinations of measurements and assumptions necessary are easily represented by a schematic diagram, such as shown in Fig. 7. If an encircled quantity is known, all quantities connected to it can be determined (the appropriate figures to be used are indicated in parentheses beside the connecting lines). Thus, when R is known, T_e/T_i can be found using Fig. 4. Once T_e/T_i is known, Fig. 6 gives the ratio σ/N, and Fig. 5 gives the ratios $\Delta f/\sqrt{T_i}$ and $\Delta f/\sqrt{T_e}$. The diagram makes it clear that when any one of the encircled quantities is known, all the others can be found. The situation where only one type of ion is present is sufficiently simple

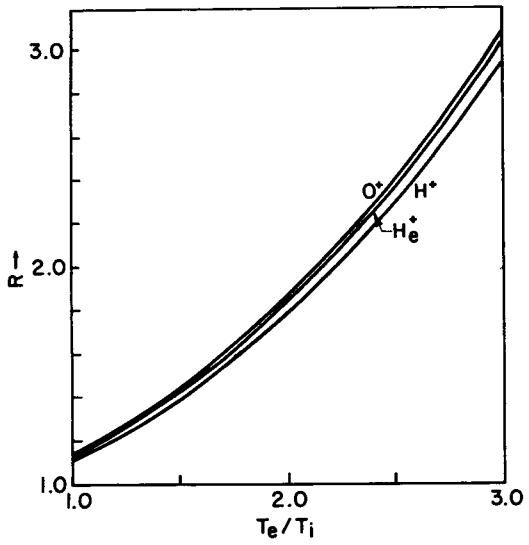

FIG. 4. PEAK-TO-CENTER RATIO R AS A FUNCTION OF T_e/T_i FOR 0^+, He^+, AND H^+.

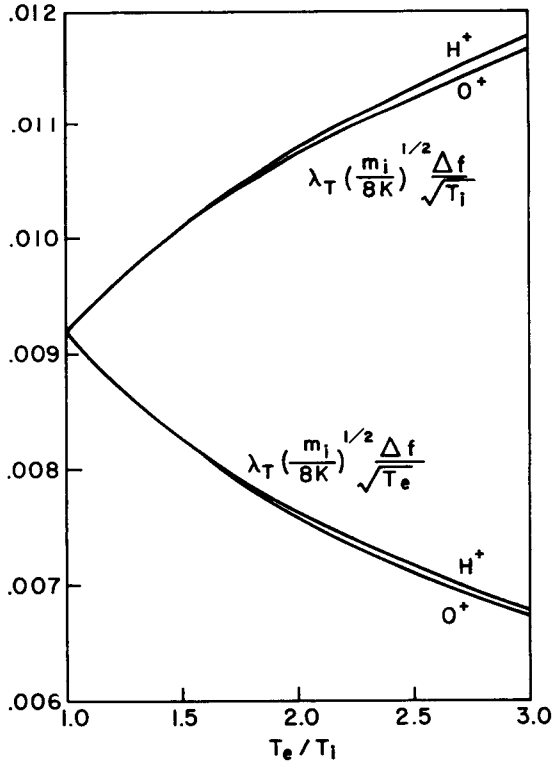

FIG. 5. VARIATION OF $\Delta f/\sqrt{T_i}$ AND $\Delta f/\sqrt{T_e}$ WITH T_e/T_i FOR 0^+ AND H^+.

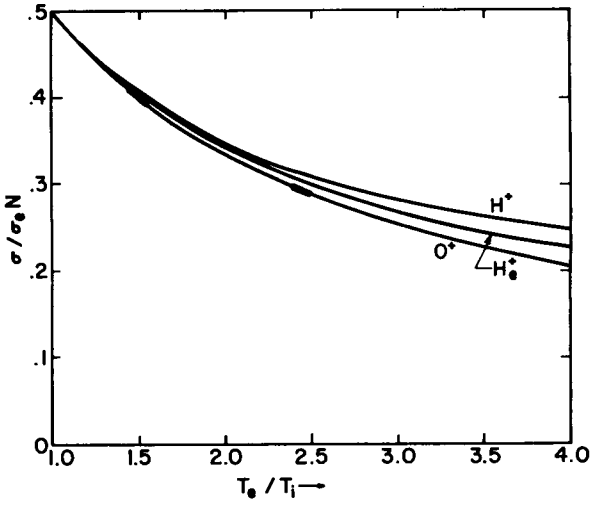

FIG. 6. σ/N AS A FUNCTION OF T_e/T_i FOR 0^+, He^+, AND H^+; σ_e IS THE POWER SCATTERED BY A SINGLE ELECTRON.

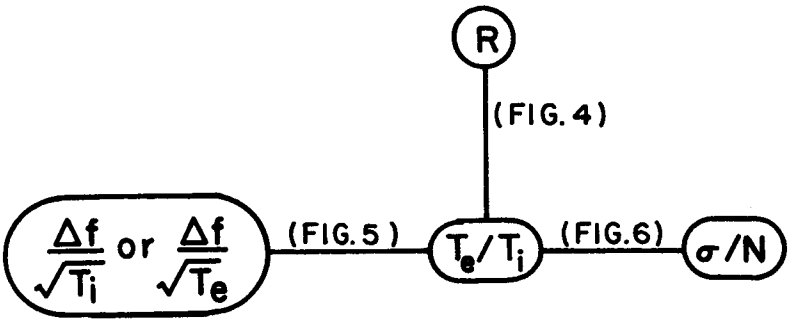

FIG. 7. INTERRELATIONS BETWEEN SCATTERING OBSERVATIONS AND CHARACTERISTICS OF IONIZED GAS WHEN ONLY ONE TYPE OF ION IS PRESENT AND ITS MASS IS KNOWN. Interrelations for 0^+, He^+, and H^+ are given in figures in parentheses.

that this diagram is probably not necessary, but it provides a concise summary of the possibilities and introduces a notation that will be helpful in examining the more complicated situations, where several types of ions are present.

With the aid of Fig. 7 we now consider the case where not all of R, Δf, and σ can be measured. Of the three, the most difficult to measure is R. If the scattering comes from sufficiently great distances the sensitivity may not be sufficient to measure R (this was the case for Evans' measurements above 400 km). Examination of Fig. 7 shows that measurements of Δf and σ must be supplemented by a measurement or assumed value of one of the other quantities before anything can be deduced, but that any one of T_e, T_i, T_e/T_i, or N will suffice. For the upper atmosphere it might be possible to make some reasonable assumption about the temperature ratio (for example, it might be reasonable to assume equilibrium conditions if the measurements were made at night), or about the ion temperature (by an assumption of an isothermal atmosphere, or by using some average values obtained from rocket measurements). Either of these assumptions would be sufficient to deduce both temperatures and the electron density from measurements of Δf and σ. If values of electron density were available, say from top- or bottom-side sounders, they could be combined with σ to give T_e/T_i, and that with Δf to give T_e and T_i.

Without a measurement of Δf, it is not possible to determine the absolute values of the temperatures; without a measurement of σ it is not possible to determine to electron density. When only σ is measured, an assumption or idependent measurement of T_e/T_i will give N (this was the approach used by Bowles [Ref. 4] to obtain electron-density profiles). Alternatively, an assumption or independent measurement of N will give T_e/T_i (this approach used by Greenhow et al [Ref. 2] to deduce T_e/T_i). When only Δf is measured, one of T_e, T_i, or T_e/T_i must be obtained by measurement or assumption, and then the others can be obtained from Δf. This method corresponds to the approach used by Evans in interpreting his observations of Δf from heights above 400 km.

III. AN IONIZED GAS CONTAINING TWO TYPES OF IONS

The interpretation of the scattering from an ionized gas containing two types of ions is considerably more complicated than when only one kind is present, and most of the discussion in this section is related to one particular example, a mixture of O^+ and He^+. This is an appropriate example for the upper atmosphere since such a mixture is likely to be the first encountered as the height of observation is increased above the F-region. While attention will be concentrated on this example, the approaches used are, in principle, applicable to the study of any ionized gas that is known to contain two particular kinds of ions.

The introduction of another ion adds a new unknown, the relative concentration of the two ionic constituents. When N_1 and N_2 are the particle densities for the two ions, then $N_1 + N_2 = N$, so the composition of the gas can be defined by the ratio N_2/N; we choose the subscript 1 to apply to the heavier constituent (in the examples this is O^+), and the subscript 2 to the lighter one (He^+ in the examples).

While the spectra for two different ions are similar in shape for a given temperature ratio (see Fig. 3), the spectra for a mixture of the two ions have shapes quite different from those for either of the ions alone. This is evident in Fig. 8, where spectra are shown for various mixtures of O^+ and He^+ for a temperature ratio of 1.5. This figure also shows that the peak-to-center ratio R is now a function of N_2/N as well as of T_e/T_i and must be represented in its dependencies as a whole family of curves rather than a single line, as it was in Fig. 4 for the case of one type of ion. Figure 9 shows R as a function of N_2/N and T_e/T_i for mixtures of O^+ and He^+.

The ratio $\Delta f/\sqrt{T_i}$, too, becomes a family of curves, shown in Fig. 10 for O^+ and He^+. The curves for temperature ratios less than 1.0 are included for use in a later discussion. Curves for $\Delta f/\sqrt{T_e}$ can be obtained from Fig. 9 by dividing $\Delta f/\sqrt{T_i}$ by $\sqrt{T_e/T_i}$.

In contrast to R and $\Delta f/\sqrt{T_i}$, σ/N changes only slightly as the composition is varied, moving smoothly from its value for the one ion to its value for the other. This change is sufficiently small to be either ignored or obtained by a simple interpolation between the curves of Fig. 6.

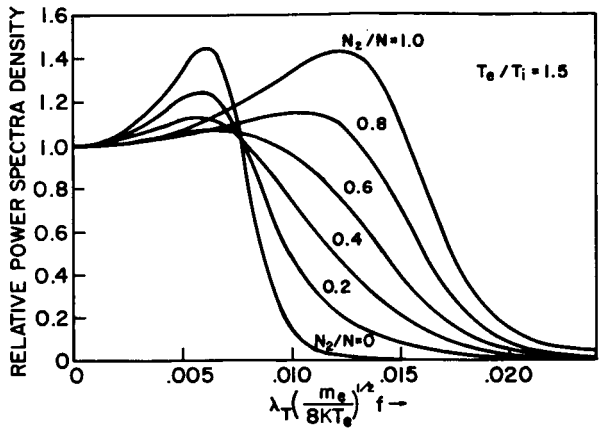

FIG. 8. SCATTERING SPECTRA FOR VARIOUS MIXTURES OF 0^+ AND He^+ WITH ELECTRON-ION TEMPERATURE RATIO OF 1.5. N_2/N is fractional concentration of He^+.

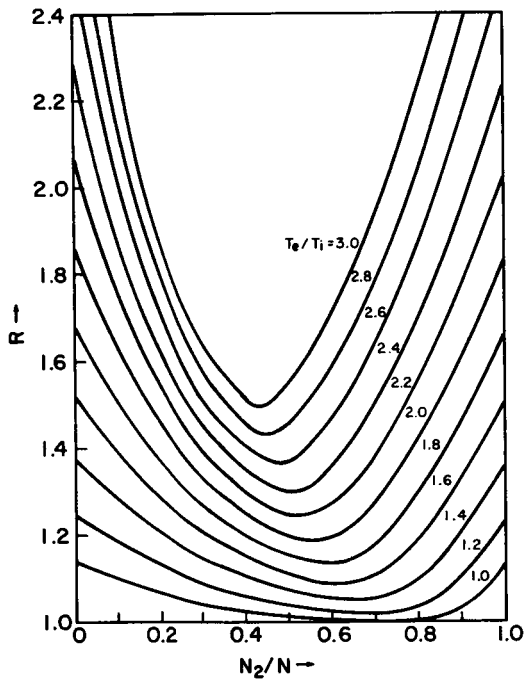

FIG. 9. PEAK-TO-CENTER RATIO R AS A FUNCTION OF T_e/T_i AND N_2/N, FOR MIXTURE OF 0^+ AND He^+.

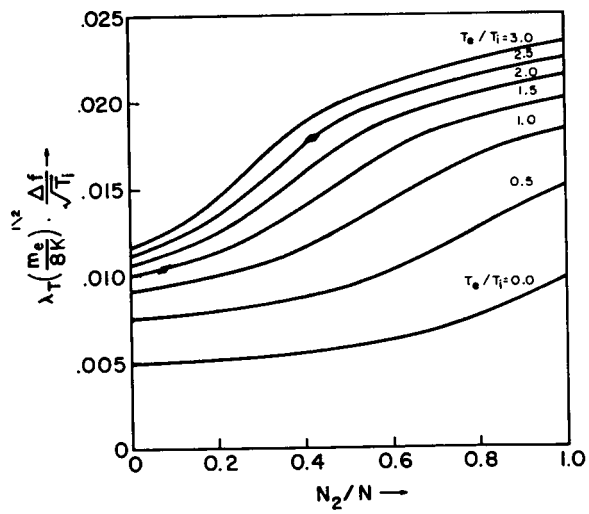

FIG. 10. DEPENDENCE OF $\Delta f/\sqrt{T_i}$ ON T_e/T_i AND N_2/N FOR MIXTURE OF 0^+ AND He^+.

Again, it is convenient to use a schematic diagram to represent the possible combinations of measurements and assumptions that can be used to determine the temperatures and densities of the electrons and ions, and the appropriate diagram is shown in Fig. 11. The quantity S is to be ignored for the moment. The hatched circle (to be referred to as a node) with the inscribed 2 indicates that when any two of the connected quantities are known, the other quantities connected to the node can be determined from that value. Thus, knowledge of R and $\Delta f/\sqrt{T_i}$ gives N_2/N and T_e/T_i (which then gives σ/N). Note that the slight dependence of σ/N on the mixture has been omitted from this diagram for clarity. In practice it can be included by using an iterative approach.

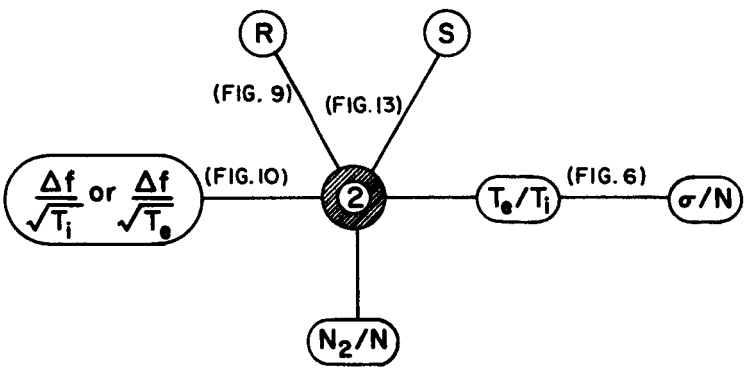

FIG. 11. INTERRELATIONS BETWEEN SCATTERING MEASUREMENTS AND TEMPERATURES AND DENSITIES FOR GAS CONTAINING TWO TYPES OF IONS. Shaded circle (node) with inscribed 2 indicates that if any two of the connected quantities are known, the others connected to the node can be determined.

Most of the possibilities arising out of consideration of Fig. 11 are readily verified by examining Figs. 6, 9 and 10. It is clear that measurement of Δf, R, and σ alone is insufficient to determine any of the temperatures or densities. However, the additional knowledge of any one of T_e, T_i, T_e/T_i, N_2/N or N will suffice to determine all the rest. For example (referring to Fig. 11), when a measurement of the electron density is available, the ratio σ/N will give T_e/T_i via

Fig. 6, which will combine with R via Fig. 9 to give N_2/N; finally, T_e/T_i and N_2/N combine via Fig. 10 to give $\Delta f/\sqrt{T_i}$, and thence T_e and T_i. It is equally clear that an assumption about T_e/T_i or N_2/N will enable all the other quantities to be determined. When T_i is known, it is necessary to use Figs. 9 and 10 simultaneously: the known values of R and $\Delta f/\sqrt{T_i}$ can be used with these figures together to determine a unique pair of values for N_2/N and T_e/T_i.

One point has been glossed over in the above discussion. In using Fig. 9 to determine N_2/N from T_e/T_i and R, it is obvious that there are really two possible values of N_2/N that will agree with the values of R and T_e/T_i. However, the ambiguity is removed by additional information of just the type available for the upper atmosphere. It is known that the amount of He^+ is very small at low heights. When a series of observations is made which extend upward from the F-region, it is obvious that only one of the two possible sets of values for N_2/N gives a continuous variation of N_2/N with height.

Another independent measurement on the spectrum is necessary if we are to deduce information about temperature and composition from scattering measurements alone. A comparison of the curves of Fig. 3 with those of Fig. 8 shows that, while the shape of the spectrum is not too different around the peak, it is much more extended in the tail of the spectrum of a gas containing He^+. It appears that some sort of measurement on the slope of the tail of the spectrum will provide information about the origin of the spectrum that is not contained in R. The actual choice of measurement would in practice often be dictated by the experimental arrangement. For illustration we choose for this new parameter S, the slope of the spectrum at the point where the power spectral density falls to one half of its central value. To keep it independent of the scales used for drawing the spectrum, we measure S on a semilogarithmic plot of the spectrum and express it as the number of decibels of change over a frequency interval f_s, as indicated in Fig. 12. Because of the type of normalizing used in defining S, it is independent of the actual temperatures and is a function of only T_e/T_i and N_2/N.

Since both R and S are functions of T_e/T_i and N_2/N, it is possible to construct a diagram, mapping the experimental measurements

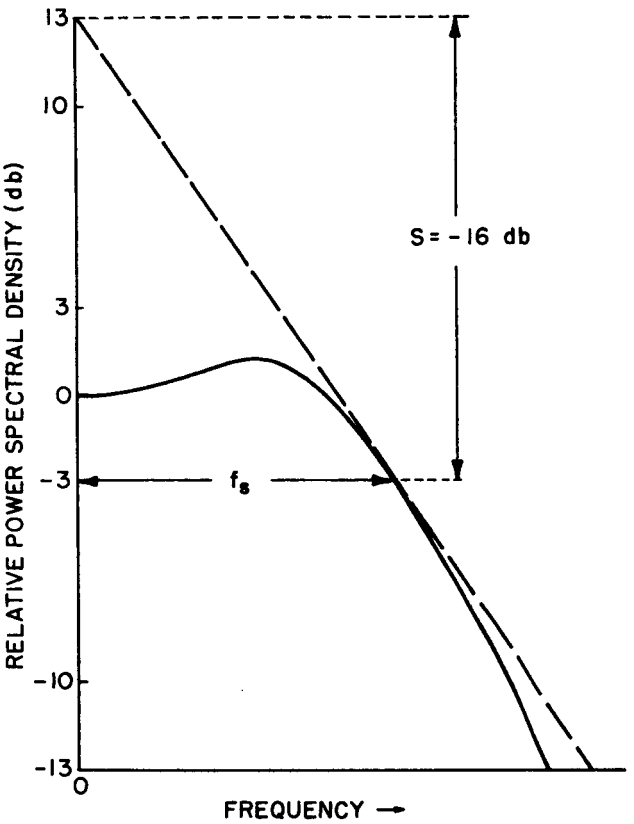

FIG. 12. DEFINITION OF PARAMETER S. f_s IS DOPPLER SHIFT TO A POINT −3 db FROM THE CENTRAL VALUE. EXAMPLE SHOWN IS FOR MIXTURE OF 0^+ AND He^+ WITH $T_e/T_i = 2.0$ AND $N_2/N = 0.3$.

of R and S into the quantities T_e/T_i and N_2/N. The portion of this mapping for temperature ratios less than 3.0 is shown in Fig. 13. Temperature ratios less than 1.0 are included for use in a later discussion. The curves for constant R in this figure are just a transformation of Fig. 9 into the new coordinates. When the curves of constant R and S are not parallel, it is possible to determine unique values for N_2/N and T_e/T_i from the point of intersection of the curves. When N_2/N is less than about 0.6 this is true, and measurements of R and S can be used to deduce values for N_2/N and T_e/T_i. Since a curve of constant S generally intersects a given curve of constant R twice, there are really two possible solutions for any pair of values of R and S (recall the ambiguity connected with Fig. 9). For atmospheric applications this presents no serious problem, since we can reasonably assume that N_2/N is a monotonic, or at least a smooth, continuous function of height.

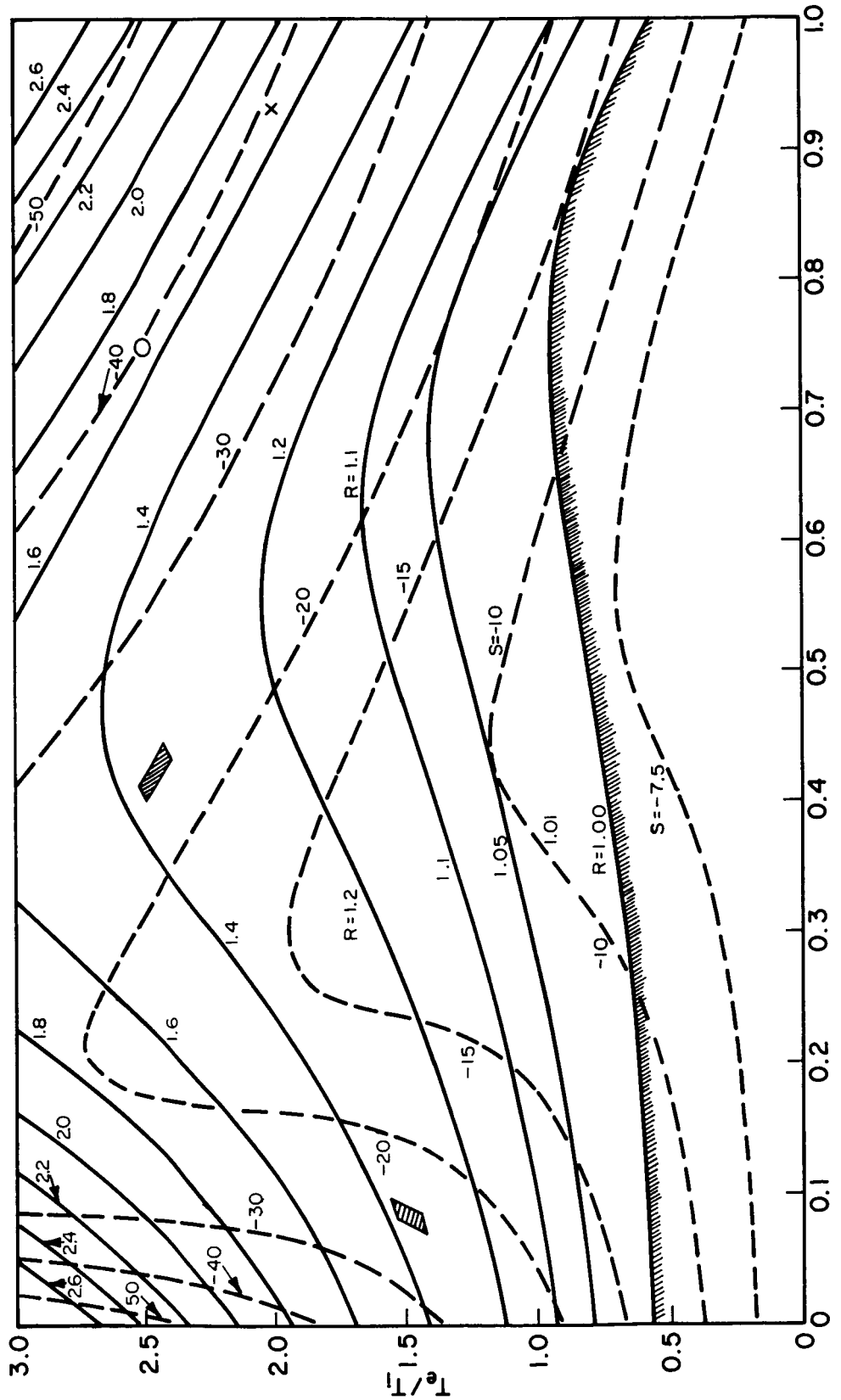

FIG. 13. MAPPING OF R AND S INTO T_e/T_i AND N_2/N FOR A MIXTURE OF 0^+ AND He^+ FOR TEMPERATURE RATIOS LESS THAN 3.0.

When N_2/N is greater than about 0.6, the curves of constant R and S become nearly parallel, implying that both quantities provide the same information about the spectrum, and it is obvious that no unique pair of values for N_2/N and T_e/T_i results. For example, if the observed values were $R = 1.3$ and $S = -30$, then, within reasonable experimental limits, the value of N_2/N could be anywhere between 0.65 and 0.90, with the corresponding values of T_e/T_i ranging from 2.0 to 1.5. Figure 14 shows that this abiguity is inherent in the shape of the spectrum. Two spectra are shown, corresponding to the O and the X on Fig. 13, near the $S = -40$ curve. The power spectral density is normalized to unity at zero doppler shift (as was done for Figs. 3 and 8); the scale for the frequency would be that indicated in parentheses, except that the scale for the $T_e/T_i = 2.0$, $N_2/N = 0.93$ curve has been multiplied by 0.898 to bring the two into superposition. The two curves are clearly indistinguishable experimentally, no matter what measurements are made on them. Incidentally, this suggests that the two parameters R and S accurately characterize the spectral shape.

The schematic diagram of interrelations is modified to include S by simply adding it to the node in Fig. 11. It must be remembered that when R and S are used as the two inputs to this node, there will be some ranges of values which do not give the other quantities connected to the node unambiguously, as has just been discussed. With this reservation it is possible, from measurements of Δf, R, S, and σ, to determine the electron and ion temperatures and densities, T_e, T_i, N_1, N_2, and N; R and S give N_2/N and T_e/T_i, which give $\Delta f/\sqrt{T_i}$. Then T_e/T_i and Δf give T_e and T_i; and T_e/T_i and σ give N.

The sequence of measurements proposed here will be of practical use only if the accuracy with which the quantities R, S, Δf, and σ must be measured to obtain reasonable estimates of the temperatures and densities is experimentally feasible. This applies in particular to R and S, since the accuracy of all deduced quantities depends on the accuracy with which R and S are measured. We will consider a typical example, where $R = 1.35 \pm 2$ percent and $S = 24$ db ± 2 percent. As has been pointed out, any pair of values of R and S leads to two possible pairs of values for T_e/T_i and N_2/N. The two solutions for

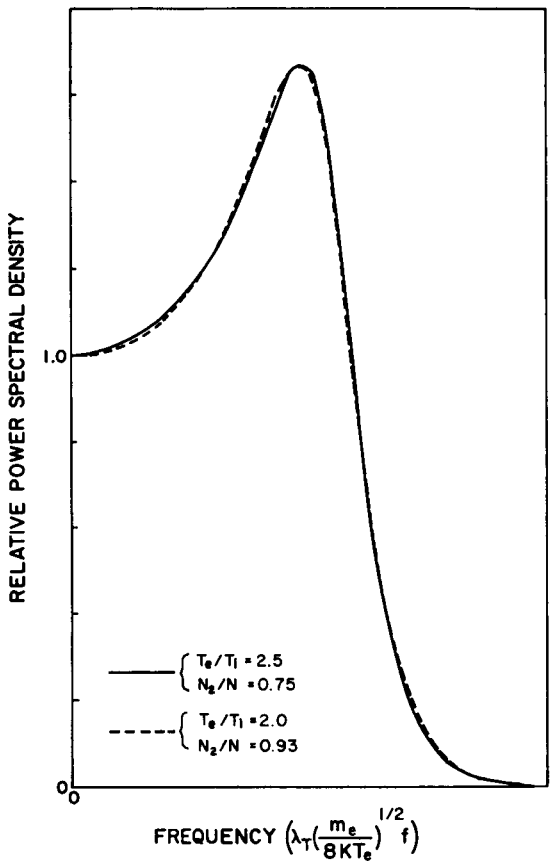

FIG. 14. TWO SPECTRA FOR MIXTURES OF O^+ AND He^+ WITH VALUES OF N_2/N AND T_e/T_i INDICATED. Frequency would be as shown in parentheses except that the scale for the $T_e/T_i = 2.0$, $N_2/N = 0.93$ curve has been multiplied by 0.898 to bring the two into superposition.

this example are shown in Fig. 13 by two hatched areas and give values of $T_e/T_i = 1.48 \pm 0.05$, $N_2/N = 8.2 \pm 1.0$ percent; and $T_e/T_i = 2.45 \pm 0.5$, $N_2/N = 42.5 \pm 2.0$ percent. In a practical situation, knowledge about the continuity of the composition in the upper atmosphere would make it clear which one of these solutions was the appropriate one. These solutions can then be used with Fig. 10 to determine $\Delta f/\sqrt{T_i}$, and thus the ion and electron temperatures. The two shaded areas on Fig. 10 correspond to the two solutions. A little calculation shows that, as a result of the uncertainty in these values for T_e/T_i and N_2/N, the deduced values for electron and ion temperatures have an uncertainty of about $\pm$ 3 or 4 percent, in addition to any uncertainty due to the accuracy of the measurement of Δf. Similarly, the two solutions are shown on Fig. 6 as shaded areas on the curve for O^+. These indicate errors in the deduced electron density of about $\pm$ 2 percent. Thus, the errors in

the deduced quantities are all of the same order of magnitude as the initial errors in R and S. At least for the case considered here, it appears that useful values for the temperatures and densities could be deduced from modest estimates of R and S.

Often it will not be possible to measure all of R, S, Δf, and σ. While the situations that arise can all be seen from an examination of Fig. 10, a few general comments may be helpful: 1) when N is to be determined, σ must be measured; 2) when temperatures are to be determined, at least one of Δf, T_i, or T_e must be measured or assumed; 3) of the nine quantities R, S, Δf, σ, T_e, T_i, T_e/T_i, N_2/N, and N, at least four must be measured or assumed if the others are to be determined.

All of the discussion on ionized gases containing two types of ions has been based on the specific example of O^+ and He^+. The characteristics of the curves given in Figs. 9, 10, and 13 depend primarily on the mass ratio of the two ions, and only very slightly on the actual masses. These figures therefore give an accurate indication of how one might study any gas containing two types of ions whose mass ratio was 4:1. In particular, a mixture of H^+ and He^+ has this mass ratio, and the approach to studying such a gas is described in its essential details by the curves given here. This has significance for the study of the upper atmosphere, since at great heights it appears likely that there will be a transition from He^+ to H^+.

For other mass ratios the character of the spectra may be quite different and, in extreme cases, a somewhat different approach might be more effective. For example, a mixture of O^+ and He^+ gives spectra of a very different shape from those for a mixture of O^+ and H^+, as will be seen in the next section (Fig. 15). Here, for a mass ratio of 16, the wide separation in frequency of the peaks for the two ions leads to spectra having very characteristic shapes, which might be interpreted in a more direct way than the method outlined here for an ion mass ratio of 4:1.

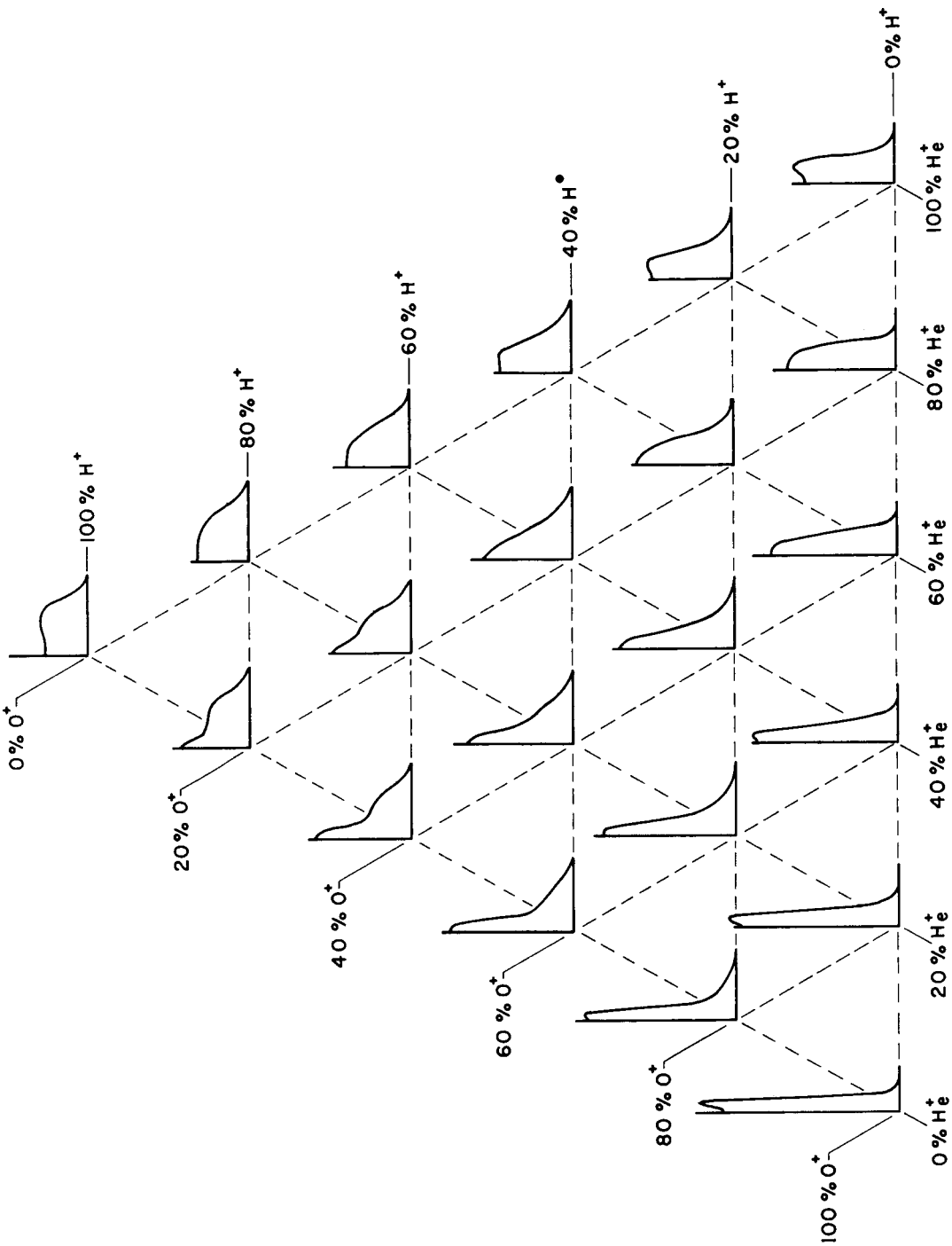

a. $T_e/T_i = 1.0$

FIG. 15. SPECTRA FOR MIXTURES OF 0^+, He^+, AND H^+. Both scales are same as used in Fig. 2.

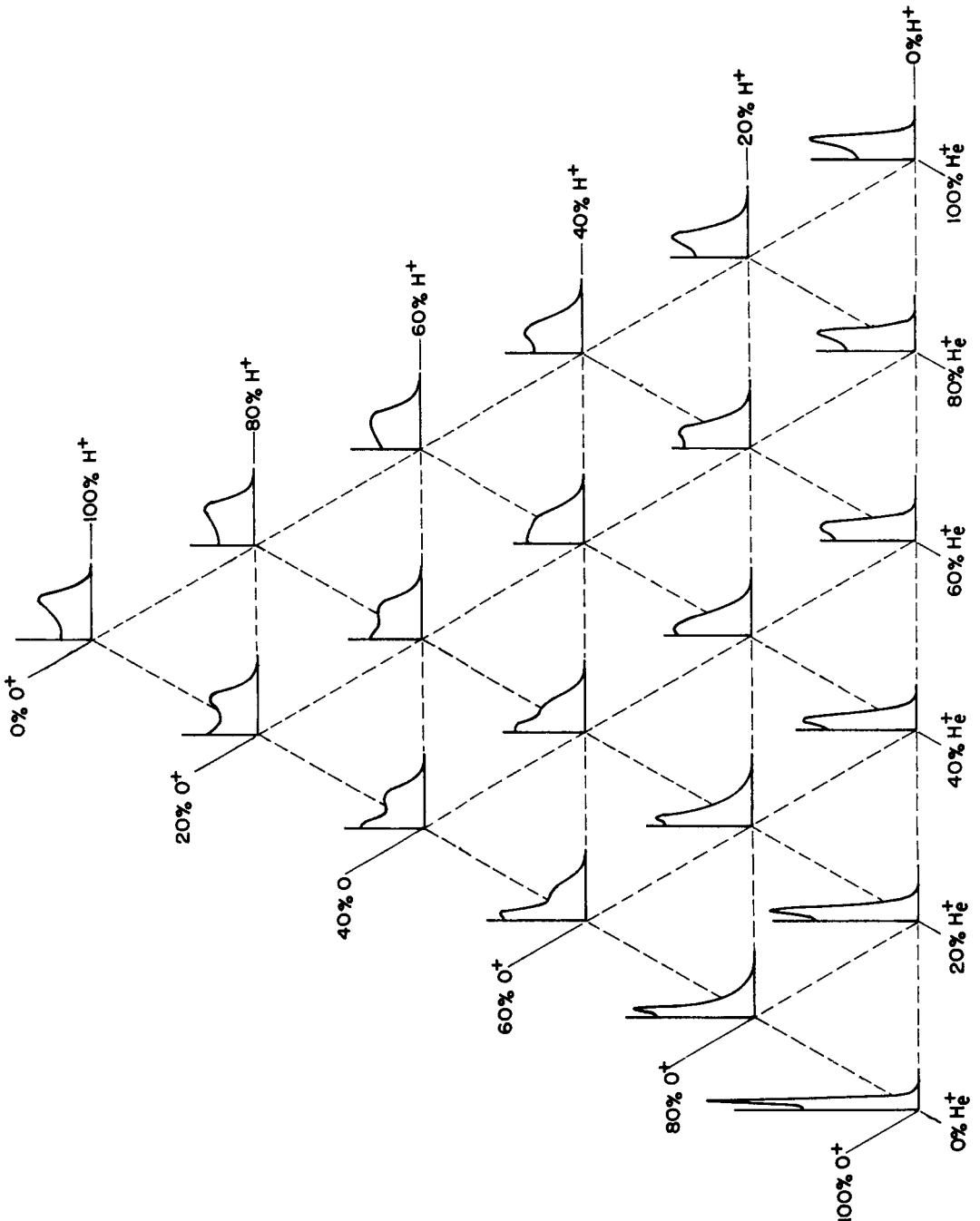
100% H+
80% H+
60% H+
40% H+
20% H+
0% H+
0% O+
20% O+
40% O
60% O+
80% O+
100% O+
100% He+
80% He+
60% He+
40% He+
20% He+
0% He+

b. $T_e/T_i = 2.0$

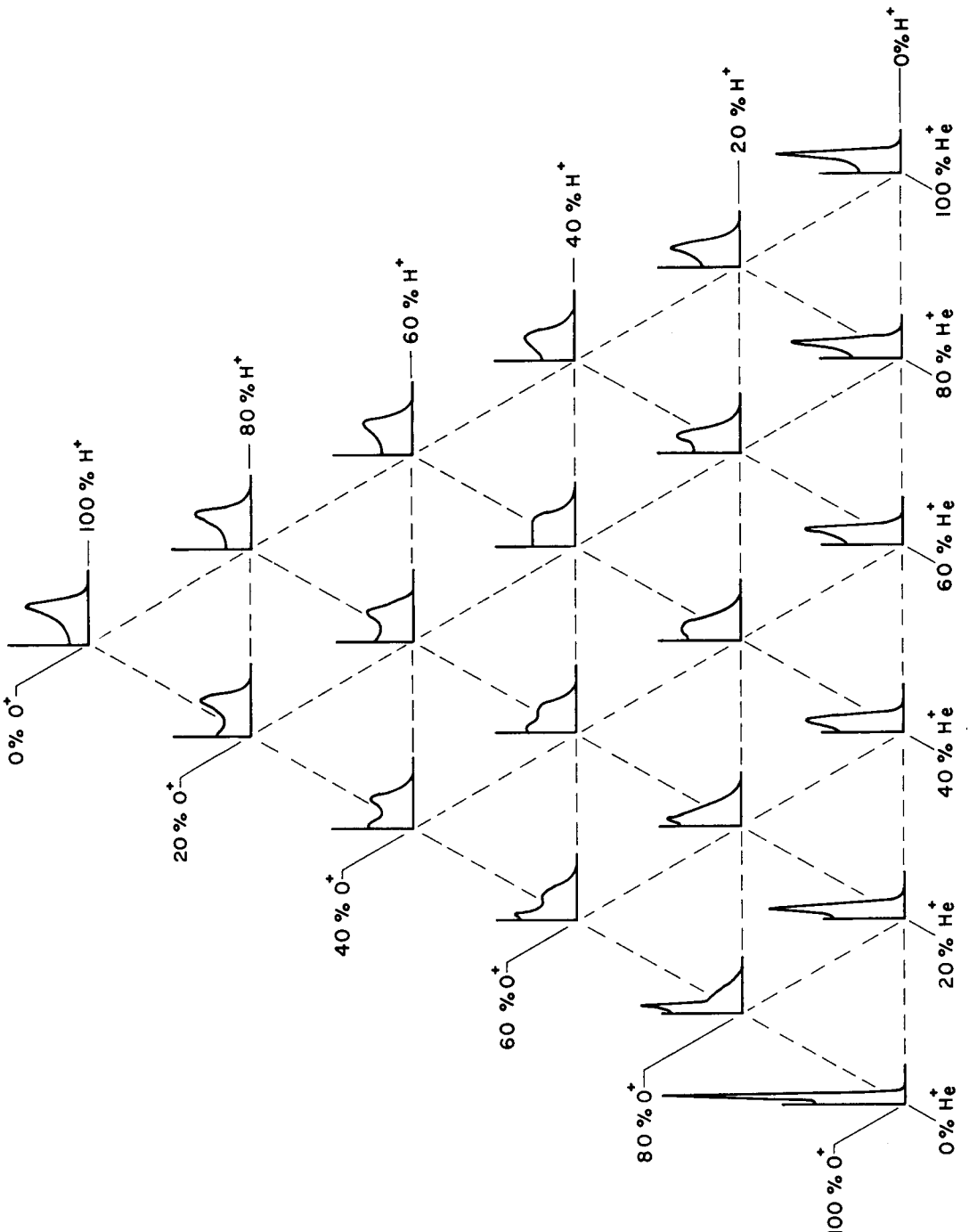
100 % H+
80 % H+
60 % H+
40 % H+
20 % H+
0% H+
0% O+
20 % O+
40 % O+
60 % O+
80 % O+
100 % O+
0% He+
20 % He+
40 % He+
60 % He+
80 % He+
100 % He+

c. $T_e/T_i = 3.0$

IV. AN IONIZED GAS CONTAINING THREE TYPES OF IONS

We consider only briefly the case where three different types of ions are present in the gas and restrict the discussion to the mixture most likely relevant to the upper atmosphere, one of O^+, He^+, and H^+. The spectra shown in Fig. 15 illustrate the effects of temperature and mixture. The scales are the same as those in Fig. 2. For high temperature ratios and small amounts of He^+ the spectra take on unusual and characteristic shapes. In these regions, it seems likely that parameters other than R and S might more directly indicate the temperature ratio and the composition of the gas. For ease in presentation, we continue to consider R and S, keeping in mind that in some cases there may be more effective ways of interpreting the spectrum.

Following the notation used for two ions, we use N_1, N_2, and N_3 for the particle densities of the three types of ions, in decreasing order of mass; since $N_1 + N_2 + N_3 = N$, we may use N_2/N and N_3/N to define the ionic compostion of the gas.

The formal relations between the various quantities are easily extended to a ternary mixture. If we are to maintain our success in determining all temperatures and densities from scattering measurements alone, we must find one more parameter to make up for the new ratio N_3/N, which we now have to determine. A study of the spectra of Fig. 15 suggests that the slope well out in the tail behaves differently from the way it behaves at the point where we measure S. Therefore we introduce another S, measured at a point -10 db from the central value, and distinguish the two by subscripts: S_3 and S_{10}. Since $\Delta f/\sqrt{T_i}$, R, S_3, and S_{10} are all functions of the temperature ratio and the composition, they are all connected to the node of the schematic diagram, which now requires at least three inputs to determine the rest of the connected quantities. The resulting schematic diagram is shown in Fig. 16.

In a general way, it is possible to indicate how measurements of the five scattering measurements might be used to determine temperatures and densities. The dependence of R on temperature ratio and mixture can be represented by surfaces of constant R in the three-dimensional space of T_e/T_i, N_2/N and N_3/N. Similar surfaces can be constructed in the

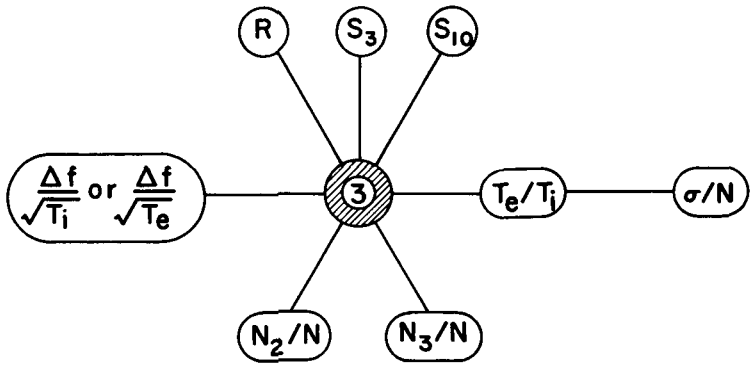

FIG. 16. INTERRELATIONS BETWEEN SCATTERING MEASUREMENTS AND TEMPERATURES AND DENSITIES FOR GAS CONTAINING THREE TYPES OF IONS. Shaded circle (node) with inscribed 3 indicates that if any three of the connected quantities are known, the other quantities connected to the node can be determined.

same space for S_3 and S_{10}. Experimental measurements of R, S_3, and S_{10} then select one surface from each of these families of surfaces. In general the surface for S_3 intersects that for R in a line L_1. The surface for S_{10} also intersects the surface for R in a different line L_2. The intersection of L_1 and L_2 defines uniquely the values of T_e/T_i, N_2/N, and N_3/N. It is quite possible that, for some ranges of the quantities R, S_3, and S_{10}, the lines L_1 and L_2 intersect in two or more points, they are nearly coincident over a range of values, or one of the lines degenerates into a surface. Under these circumstances it would not be possible to deduce uniquely the temperature ratio and densities from the measurements. The extensive calculations necessary to locate ambiquities have not been carried out, but the limited study that has been made indicates that, for a least some regions, it is possible to obtain a unique interpretation. In practice, it would be a very arduous task to compute the lines L_1 and L_2 for each set of measurements obtained. A more feasible approach might involve using a computer to search for the values of T_e/T_i, N_2/N, and N_3/N for the best fit to

the measurements of R, S_3, and S_{10}. The rest of the interpretation, involving Δf and σ, is straightforward, being identical in principle to the approach used for an ionized gas with two types of ions.

Since it is not known what model really applies to the upper atmosphere, it is not possible to determine beforehand the height range over which only O^+ and He^+ are present in significant quantities. Therefore, it is important to be able to distinguish between mixtures containing varying proportions of He^+ and H^+ in a preponderance of O^+. Preliminary calculations verify what is suggested by the spectra in Fig. 15—that if S_{10} or its equivalent can be measured, an unambiguous interpretation of mixtures of this type can be obtained. Whether He^+ or H^+ is dominant as the minor constituent should be evident from even a cursory examination of the tail of the spectrum.

V. THE EFFECT OF kD ON THE INTERPRETATION

Throughout this discussion it has been assumed that the transmitted wavelength is very much larger than the Debye length. At vhf this condition is not strictly true for scattering from sufficiently great heights. It is therefore necessary to consider the effect of kD on the spectral shape and thus on the interpretation. An examination of the analytical expression for the spectrum for an ionized gas containing one type of ion suggests that, for values of kD less than 1.0, the spectral shape is the same for $kD \ll 1$, but with a temperature ratio $(T_e/T_i)/[1 + (kD)^2]$. Numerical computations have verified this similarity for mixtures of O^+ and He^+, and for $kD \leq 1$. Even when $kD = 1.0$, the temperature transformation gives values for R and S that are too low by only 1 or 2 percent. For convenience in the rest of this discussion, we denote quantities deduced on the assumption that $kD \ll 1$ by a prime. Thus, when T_e/T_i is the true temperature ratio, and $(T_e/T_i)'$ is that deduced on the assumption that $kD \ll 1$, then

$$T_e/T_i = [1 + (kD)^2]\ (T_e/T_i)' \qquad (kD \leq 1).$$

Note, in particular, that the value of N_2/N deduced on the assumption of $kD \ll 1$ is correct, independent of the value of kD (for $kD \leq 1$). The width of the spectrum is affected by the value of kD in such a way that, for $kD \leq 1$, the value of T_i deduced from Fig. 10 using $(T_e/T_i)'$ and N_2/N is still correct. The value of σ/N is affected in a different way by kD than these other quantities. In Fig. 17 the variation of σ/N with T_e/T_i and kD is shown for 100-percent O^+.

Consider a mixture of O^+ and He^+, and suppose that measurements of R, S, Δf, and σ are available for a situation where kD is not very small, but less than 1.0. Figure 13 can be used to obtain $(T_e/T_i)'$ and N_2/N. Although T_e/T_i is unlikely to be less than 1.0, the value of $(T_e/T_i)'$ may be as small as 0.5, and for this reason values of T_e/T_i less than 1.0 have been included in Fig. 13. Note that the value of R is 1.0 everywhere below the hatched line $R = 1.0$. Figure 10 will then give T_i, and from Fig. 17, using σ and $(T_e/T_i)'$, we can deduce a

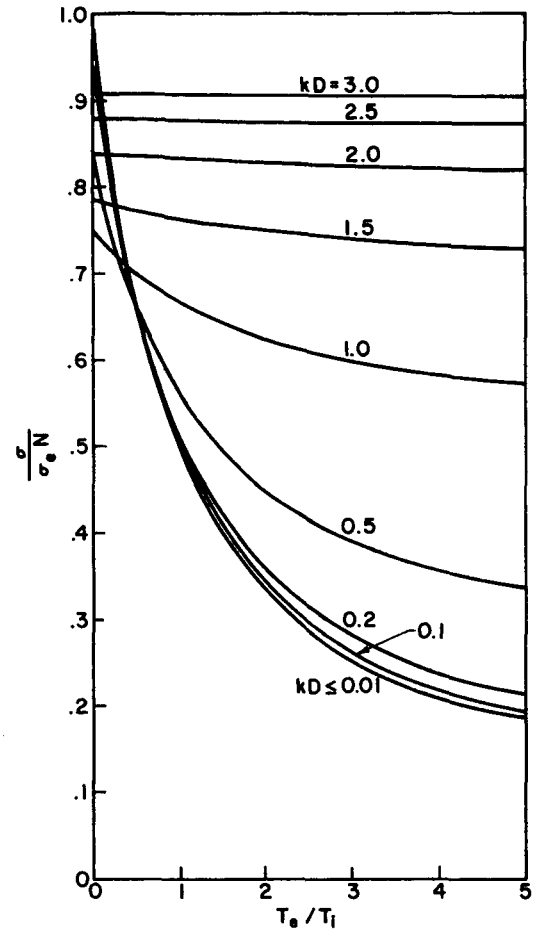

FIG. 17. σ/N AS A FUNCTION OF T_e/T_i FOR VARIOUS VALUES OF kD. σ_e is the power scattered by a single electron.

value for the electron density N'. Based on the assumption of kD << 1, we can find an estimate for the correct value of kD' from the expression

$$(kD)' = 69.1 \sqrt{(T_e/T_i)' \quad T_i/N'} = 69.1 \sqrt{T_e'/N'}.$$

It would then be possible to find a new estimate for T_e/T_i by using this new value of kD (instead of the assumption that kD << 1); several iterations would eventually converge on the correct values for kD and T_e/T_i. However, it is possible to calculate directly the relation between the values $(kD)'$ and $(T_e/T_i)'$, and kD and T_e/T_i, and this relation is shown in the curves of Fig. 18 for values of T_e/T_i up to 3.0 and values of kD up to 1.5. By the use of this diagram, the extension of the technique up to kD = 1.0 is, at least in principle, quite

straightforward. Notice, however, that it is now essential to measure all four scattering quantities, in order to be able to obtain initial estimates of kD.

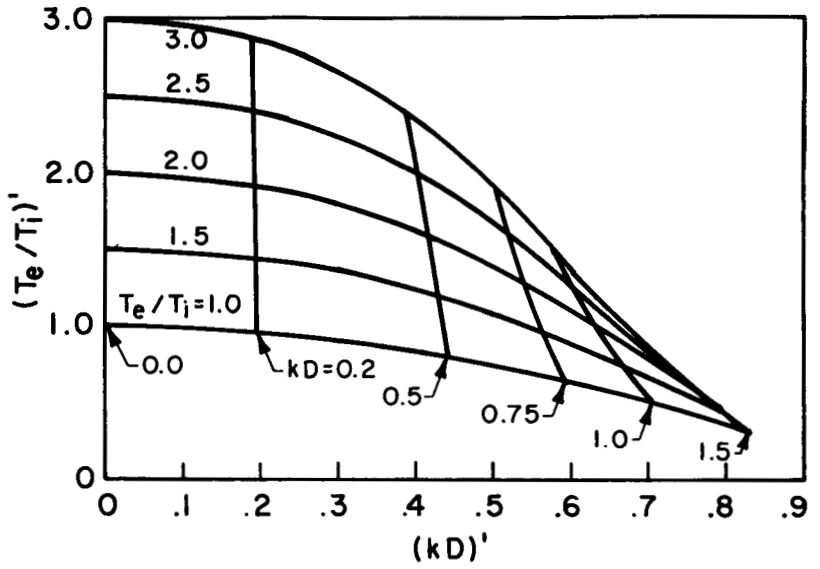

FIG. 18. TRANSFORMATION FROM $(T_e/T_i)'$ AND (kD)' TO T_e/T_i AND kD. Primed quantities are those calculated on the assumption that $kD \ll 1$. Unprimed quantities are the true values.

Figures 13 and 18 indicate another difficulty that limits the practical range of kD to values less than about 0.75. When kD = 1.0, the apparent temperature ratios, corresponding to true temperature ratios between 1.0 and 2.0, are between 0.5 and 1.0 (Fig. 18). From Fig. 13 it can be seen that the values of R for this entire range of temperatures are nearly equal to 1.0, so that extremely accurate measurements of R would be necessary to obtain meaningful values for temperature ratio and density. At low enough apparent temperature ratios the peak of the spectrum is at the center (zero doppler shift). On Fig. 13 this is everywhere below the R = 1.0 line, and a measurement of R and S could not be used to obtain T_e/T_i and N_2/N without some subsidiary assumptions.

For the purposes of illustration we will take the value $kD = 0.75$ as representing the maximum value of kD for which the interpretation is reliable. The electron density at which this value of kD occurs is shown in Fig. 19 as a function of frequency, for electron temperatures of 1000, 2000 and 3000 ^{o}K. Also shown is the electron density at which $kD = 0.1$. When kD is less than this value, the corrections due to kD are less than 1 percent, and in most cases could be neglected. From Fig. 19 we see that, at 50 Mc, the effect of kD can be ignored when the electron density is greater than about 4×10^9 el/m^3, and can be easily corrected for until the electron density is less than 6×10^7 el/m^3. The first of these densities might be encountered in the upper atmosphere at heights of 800 to 2000 km, while the second might not be encountered even at heights of tens of thousands of kilometers. At 400 Mc, the effect of kD becomes important at densities of about 2×10^{11} el/m^3, which might be encountered as low as 300 km during the night. The effect of kD can be corrected for until the electron density is less than about 4×10^9 el/m^3, which might be encountered at heights of 1000 or 2000 km, but could occur as low as 800 or 900 km.

It is clear that the effect of kD can not be ignored when observations are made at a frequency as high as 400 Mc. If observations are extended to thousands of kilometers (where mixtures of ions are important), a frequency of 50 Mc would be much more desirable than higher frequencies, where the large values of kD at these heights would make the interpretation of the spectra in terms of the ionic composition and temperatures difficult or impossible.

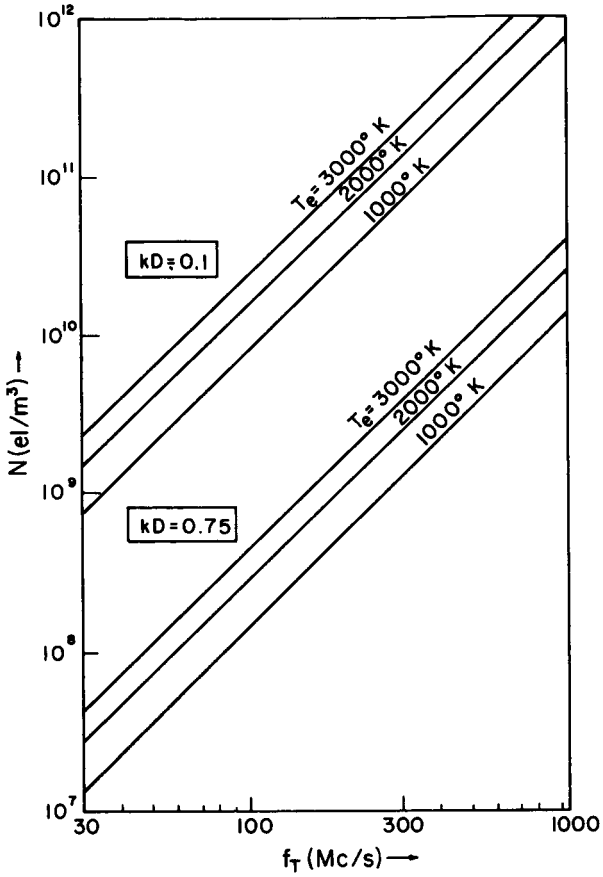

FIG. 19. ELECTRON DENSITIES AND TRANSMITTED FREQUENCIES THAT GIVE VALUES OF kD OF 0.1 AND 0.75, FOR ELECTRON TEMPERATURES OF 1000, 2000 AND 3000 °K.

VI. CONCLUSIONS

Ionic mixtures and temperature non-equilibrium of the electrons and ions in the ionosphere and magnetosphere complicate the interpretation of radar observations of electron scattering. The effects of ionic mixtures probably become significant at heights as low as 600 to 1000 km. On the basis of the model of Bauer [Ref. 10], the first mixture to be encountered with increasing height will be one of O^+ with a smaller amount of He^+. The analysis given in this paper shows that measurements of the spectral shape for electron scattering together with the total scattered power per unit volume will give unambiguously the electron and ion densities and temperatures for such mixtures. Significant amounts of H^+ may also be present in this region. It appears to be possible, with sufficiently sensitive measurements, to determine the relative proportions of He^+ and H^+ in a preponderance of O^+, and thus determine densities for all three ions as well as the electron and ion temperatures in the lower part of the magnetosphere.

The effectiveness of the technique also depends on the magnitude of kD, which, if not sufficiently small, will further complicate the interpretation of the measurements. It appears that at low vhf frequencies the effects of kD can be corrected for throughout the magnetosphere. However, at low uhf frequencies, the value of kD may be sufficiently large above heights as low as 800 km to make interpretation of the spectra in terms of ion properties difficult or impossible.

REFERENCES

1. J. V. Evans, "Diurnal Variation of the Temperature of the F Region," J. Geophys. Res., 67, 1962, pp. 4914-4920.
2. J. S. Greenhow, H. K. Sutcliffe, and C. D. Watkins, "The Electron Scattering Cross-Section in Incoherent Backscatter," J. Atmospheric Terrest. Phys., 25, 1963, pp. 197-207.
3. V. C. Pineo, L. G. Kraft, and H. W. Briscoe, "Some Characteristics of Ionospheric Backscatter Observations at 440 Mc/s," J. Geophys. Res., 65, 1960, pp. 2629-2633.
4. K. L. Bowles, "Profiles of Electron Density over the Magnetic Equator Obtained Using the Incoherent Scatter Technique," NBS rpt. no. 7633, National Bureau of Standards, Boulder, Colorado, and the Instituto Geofisico del Peru, Lima, Peru, 18 Dec 1962.
5. K. L. Bowles, "Incoherent Scattering by Free Electrons as a Technique for Studying the Ionosphere and Exosphere: Some Observations and Theoretical Considerations," J. Res. NBS, 65D, 1961, pp. 1-14.
6. J. A. Fejer, "Scattering of Radio Waves by an Ionized Gas in Thermal Equilibrium in the Presence of a Uniform Magnetic Field," Can. J. Phys., 39, 1961, pp. 716-740.
7. T. Hagfors, "Density Fluctuations in a Plasma in a Magnetic Field, with Applications to the Ionosphere," J. Geophys. Res., 66, 1961, pp. 1699-1712.
8. K. L. Bowles, Discussion at Spring URSI meeting, Washington, D.C., Apr 1963.
9. H. Carru, R. Benoit, and M. Petit, "La diffusion incohérente nouvelle méthode d'étude de l'ionosphère à partir du sol," La Nature: Science Progres, No. 3330, Oct 1962, pp. 422-429.
10. S. J. Bauer, "Helium Ion Belt in the Upper Atmosphere," Nature, 197, 1963, pp. 36-37.
11. D. R. Moorcroft, "On the Power Scattered from Density Fluctuations in a Plasma," J. Geophys. Res., 68, 1963, pp. 4870-4872.

DISTRIBUTION LIST
for
U.S. Air Force Contract AF19(604)-7436

1 AF Ballistic Missile Division (WDSOT)
Air Force Unit Post Office
Los Angeles 45, Calif.

1 Hq. AFCRL, OAR (CRW)
L.G. Hanscom Field
Bedford, Mass. 01731

1 Hq. AFCRL, OAR (CRD)
L.G. Hanscom Field
Bedford Mass. 01731

1 Hq. AFCRL, OAR (CRB)
L.G. Hanscom Field
Bedford, Mass. 01731

1 ESD (ESRDW) Major J. Hobson
L.G. Hanscom Field
Bedford, Mass. 01731

1 ASD (ASRNRE-3)
Wright-Patterson AFB, Ohio
Attn: Mr. Paul Springer

1 AFSC, SCTAE
Andrews AFB, Washington, D.C.
Attn: Lt. Col. E. Wright

1 USASRDL
Institute for Exploratory Res.
Evens Avenue
Ft. Monmouth, N.J.
Attn: Dr. Fred B. Daniels

1 U.S. Army Signal Radio Propagation Agency
Ft. Monmouth, N.J.
Attn: Mr. Frederic H. Dickson, Chief

1 Asst. Sec. of Def., R and D
Info. Office Library Branch
Pentagon Bldg.
Washington 25, D.C.

1 Department of Astronomy
University of Sydney
Sydney, Australia
Attn: Dr. B.Y. Mills

1 Officer in Charge
Radio Res. Board Lab.
School of Electrical Eng.
University of Sydney
Sydney, N.S.W., Australia
Attn: Dr. G.H. Munro

1 CSIRO
Sydney, Australia
Attn: Librarian

1 Dominion Radio Astrophysical Observatory
Box 248
Penticton, B.C., Canada

1 Jodrell Bank Experimental Station
Lower Withington, Macclesfield
Cheshire, England
Attn: Mr. G. Taylor

1 Mullard Radio Astronomy Observatory
Cavendish Laboratory
Cambridge, England

1 Laboratoire National De Radio Electricite
196 Rue de Paris
Bagneaux
Paris, France

1 Laboratory of Physics of the Atmosphere
1 Quai Branly
Paris VII, France
Attn: Professor E. Vassy

1 Ionospheric Institute of Breisach
Breisach, W. Germany
Attn: Professor K. Rawer

Universitats - Sternwarte
1 Bonn, Germany

Laboratory of Electronics
University of Athens
Solonos Street 104
Athens, Greece
1 Attn: Prof. M. Anastassiades, Director

Centro Microonde
Via Panciatichi, 56
Florence, Italy
1 Attn: Prof. Nello Carrara, Director

Radio Research Laboratories
Kokibunji P.O. Koganei-shi
1 Tokyo, Japan

Kyoto University
Kyoto, Japan
1 Attn: Prof. T. Obayashi

Sterrewacht
1 Leiden, Netherlands

Norwegian Defense Research Establishment
Kjeller, Norway
1 Attn: Dr. B. Landmark

Kiruna Geiphysical Observatory
Kiruna, Sweden
1 Attn: Dr. Bengt Hultqvist

Radio Research Board Laboratory
The University of Sydney
1 Sydney, Australia

National Bureau of Standards
Boulder, Colorado
1 Attn: Librarian

Radio Communication and Systems Division, 85.00
Central Radio Propagation Lab.
National Bureau of Standards
Boulder, Colorado
1 Attn: R.C. Kirby

Federal Communications Commission
Technical Research Division
Washington 25, D.C.
1 Attn: Mr. Harry Fine

Office of Science
Office of the Asst. Sec. of Def., R and E
1 Washington 25, D.C.

Smyth Research Associates
3555 Aero Court
Research Park
1 San Diego 11, Calif.

STL Technical Library
Documents Acquisitions
Space Technology Laboratories, Inc.
P.O. Box 95001
1 Los Angeles 45, Calif.

Raytheon Company
225 Crescent Street
Waltham, Mass.
1 Attn: Mr. D.A. Hedlund, Com. and Data Proc. Operation

Cornell Aeronautical Laboratory, Inc. of Cornell Univ.
4455 Genesee Street
Buffalo 21, N.Y.
1 Attn: Dr. Walter Flood

Naval Research Laboratory
1 Washington, D.C.

Chief of Naval Research
Electronics Branch (Code 427)
Department of the Navy
Washington 25, D.C.
1 Attn: Dr. Arnold Shostak

Radio Astronomy Observatory
California Institute of Technology
1 Owens Valley, Calif.

Department of Physics
University of California
Berkeley, Calif.
1 Attn: Dr. R.R. Brown

Radio Astronomy Observatory
University of California
1 Hat Creek, Calif.

Stanford Research Institute
Menlo Park, Calif.
1 Attn: Dr. Allen M. Peterson

High Altitude Observatory
University of Colorado
Boulder, Colorado
1 Attn: Librarian

Yale University Observatory
1 Bethany, Conn.

Georgia Technology Res. Inst.
Eng. Experiment Station
722 Cherry Street, N.W.
Atlanta, Georgia
1 Attn: W.B. Wrigley, Head
Communications Branch

Radio Astronomy Observatory
University of Illinois
1 Danville, Illinois

Dept. of Physics and Astronomy
State University of Iowa
1 Iowa City, Iowa

Dept. of Terrestrial Magnetism
Carnegie Inst. of Washington
1 Derwood, Md.

Dept. of Physics and Astronomy
University of Maryland
College Park, Md.
1 Attn: Dr. Gart Westerhout

Agassiz Station
Harvard University
1 Harvard, Mass

Harvard College Observatory
60 Garden Street
Cambridge, Mass.
1 Attn: Librarian

Millstone Hill Observatory
Lincoln Laboratory
1 Westford, Mass.

Massachusetts Institute of
Technology
Laboratory of Electronics
Cambridge, Mass.
1 Attn: Dr. A.H. Barrett

Massachusetts Institute of
Technology
Lincoln Laboratory
P.O. Box 73
Lexington 73, Massachusetts
1 Attn: Mr. J.H. Chisholm - C-357

The University of Michigan
Engineering Research Institute
Willow Run Laboratories
Will Run Airport
Ypsilanti, Mich.
1 Attn: Librarian

The Radio Astronomy Observatory
University of Michigan
1 Dexter, Michigan

School of Physics
University of Minnesota
Minneapolis, Minn.
1 Attn: Dr. J.R. Winckler

Sacramento Peak Observatory
Sunspot, N.M.
1 Attn: Dr. John Evans

Cornell University
School of Electrical Engineering
Ithaca, N.Y.
1 Attn: Dr. W. Gordon

Cornell University
Center for Radiophysics and
Space Research
1 Ithaca, N.Y.

Department of Physics
Rensselaer Polytechnic Institute
Troy, N.W.
1 Attn: Dr. R. Fleischer

Ohio State University
1314 Kinnear Road
Columbus 12, Ohio
1 Attn: Dr. John Kraus

Radio Astronomy Station
Harvard College Observatory
Harvard University
1 Ft. Davis, Texas

University of Texas
Elec. Eng. Research Laboratory
Box 8026, University Station
Austin 12, Texas
1 Attn: Prof. A.W. Straiton

National Radio Astronomy
Observatory
1 Greenbank, West Virginia

Hq. AFCRL, OAR
L.G. Hanscom Field
Bedford, Mass. 01731
10 Attn: Richard S. Allen, CRFR

A.U. Library
1 Maxwell AFB, Alabama

Hq. AFCRL, OAR (CRTPM)
L.G. Hanscom Field
1 Bedford, Mass. 01731

AFCRL, OAR (CRXRA) Stop 39
L.G. Hanscom Field
5 Bedford, Mass. 01731

Hq. USAF (AFRST)
1 Washington 25, D.C.

Hq. AFCRL, OAR
L.G. Hanscom Field
Bedford, Mass. 01731
1 Attn: M.B. Gilbert, CRTE

Scientific and Technical
Information Facility
Bethesda, Md.
1 Attn: NASA Representative (S-AK-DL)

Defense Documentation Center (DDC)
Cameron Station
10 Alexandria, Va.

Documents Expediting Project
(Unit X)
Library of Congress
1 Washington 25, D.C.